Zeng *et al. Stem Cell Research & Therapy* (2025) 16:114
https://doi.org/10.1186/s13287-025-04240-6

Stem Cell Research & Therapy

RESEARCH Open Access

Lipid droplet-free nanovesicles extruded from stromal vascular fraction improve adipocyte regeneration in the centre of dermal graft

Yuyang Zeng[1,2†], Di Sun[1,3†], Rongrong Wang[1,3], Ran An[1,3], Jiaming Sun[1,3*] and Jie Yang[1,3*]

Abstract

Background The stromal vascular fraction (SVF) has been validated for enhancing tissue regeneration because of its concentration of multipotent cells and growth factors, and for mitigating inflammatory response due to its elimination of the majority of lipid droplets. However, it is difficult for fresh SVF to maintain bioactivity for a long period, and the loss of numerous tangible masses during preparation limits its application in repairing large volume defects. Here, we fabricated a self-assembly nanovesicle extruded from SVF (SVF-EVs) by mechanical shear and co-transplanted it with dermal microparticles to verify its potential for repairing large volume defects.

Methods The SVF-EVs were prepared by removing the oil from adipose tissue followed by sequentially extruding SVF through membrane filters. The lipid content of SVF-EVs was compared with SVF using Oil Red O staining. The morphology and adipogenic-related protein of SVF-EVs were characterized. The pro-adipogenic potency of SVF-EVs in vitro was determined using Oil Red O staining of ADSCs, western blot, and qRT-PCR. In vivo, dermal particle grafts mixed with SVF-EVs were subcutaneously transplanted in nude mice and harvested after 4 and 6 weeks. By examining the weight and volume of grafts and histological staining, we explored the effect of SVF-EVs on adipose tissue regeneration and anti-inflammatory ability.

Results Our results showed that the removal rate of proceeding of SVF-EVs could remove 75.07 ± 2.80% lipid in SVF. The SVF-EVs displayed 100 ~ 150 nm sphere vesicles and contained pro-adipogenic protein. In vitro, SVF-EVs promote the synthesis of lipids in ADSCs. Besides, after co-transplanting of SVF-EVs, adipose regeneration was detected in vivo in the dermal particle grafts.

Conclusions These findings revealed that extruding SVF into nanovesicles can effectively reduce the implantation of lipid droplets that cause inflammation, and co-transplanting SVF-EVs with dermal microparticles may be a considerable strategy for large volume defects repair.

†Yuyang Zeng and Di Sun contributed equally to this work.

*Correspondence:
Jiaming Sun
sunjiaming@hust.edu.cn; sunjm1592@sina.com
Jie Yang
abrams18@163.com

Full list of author information is available at the end of the article

Keywords Nanovesicles, Stromal vascular fraction, Adipocyte regeneration, Lipid droplet, Inflammation

Introduction

Previous researches have demonstrated that the peripheral regions of fat grafts exhibit higher survival rates, a phenomenon attributed to oxygen infiltration from the surrounding environment [1–3]. In contrast, adipocytes located in the central area experience hypoxic conditions, ultimately resulting in their necrosis and subsequent dissolution [4]. This process is accompanied by the release of lipid droplets, which induces an inflammatory response at the recipient site [5]. Subsequently, M1-type macrophages migrate to the site and phagocytize the released oil droplets, whereas M2-type macrophages facilitate the remodeling of the extracellular matrix [6]. These processes not only hinder neovascularization but also enhance mechanical strength while reducing adipogenesis [7, 8]. According to Yoshimura et al., the equilibrium between adipocyte regeneration and necrosis significantly affects the volume retention rate [9]. Consequently, decreasing the proportion of lipid droplets within the graft is advantageous for improving the volume retention rate.

Adipose-derived stem cells (ADSCs) have demonstrated the ability to influence macrophage polarization, promote endothelial cell migration, facilitate extracellular matrix remodeling, and differentiate into adipocytes [10, 11]. Strategies focused on the use of ADSCs assistance, combined with the depletion of implanted lipid droplets, have attracted significant attention in the field of fat grafting [10, 12, 13]. The stromal vascular fraction (SVF), a heterogeneous cell population extracted from adipose tissue, comprises ADSCs, endothelial cells, pericytes, and other cellular constituents. The high concentration of stem cells within SVF has contributed to its widespread application in tissue regeneration [14]. Lu et al. developed a hybrid gel, referred to as SVF-gel, which incorporates extracellular matrix components with SVF cells [15]. This innovative method significantly diminished the substantial lipid droplet content of adipocytes via mechanical shearing forces, demonstrating considerable potential for clinical applications [16, 17].

Nevertheless, researchers highlighted a significant limitation: the volumetric capacity of SVF-gel constitutes only 10–15% of the original adipose tissue, thereby considerably constraining the injectable volume [18]. Moreover, existing literature indicate the difficulties in preserving and reusing SVF, primarily attributed to its intrinsic cellular activity [19, 20]. This necessitates the immediate use of SVF following its preparation, thereby substantially increasing the operational complexity and time sensitivity of the entire procedure.

The liposome-like structure of nanovesicles demonstrates a capacity to stabilize and safeguard the biological activity of their contents, thereby offering novel strategies for addressing the aforementioned challenges [21]. Yoon et al. described a technique involving cell membrane fragmentation and self-assembly, which entails the sequential extrusion of cells through microfilters, resulting in the generation of a multitude of vesicles encapsulating various bioactive components [22]. Researchers have developed a diverse array of nanovesicles, identifying their potential applications in drug delivery, tumor diagnosis, and various other fields. For instance, Liu et al. encapsulated photodynamic drugs within self-assembled nanovesicles derived from red blood cells. This approach leverages the prolonged retention of red blood cells within the body to protect the drugs from rapid clearance [23]. Wen et al. conducted a comparative analysis of eight additional cancer cell lines, revealing a significant similarity in membrane protein composition between natural extracellular vesicles and self-assembled nanovesicles [24]. This finding suggests a promising avenue for advancements in cancer diagnosis and immune-chemotherapy. The top-down bioengineering approach employed, which involves the conversion of cells into vesicles via sequential extrusion, disrupts cellular membranes and theoretically enables the isolation and removal of lipid droplets stored within adipocytes. It can be postulated that the SVF, following this top-down procedure, may prevent the formation of oil cysts and enhance fat regeneration within the graft, as a result of the removal of lipid droplets. Nonetheless, there has been a paucity of research examining the outcomes of SVF following sequential extrusion. In our prior study, SVF derived from adipose tissue underwent repeated shear through a filter membrane to yield nanoscale vesicles. These vesicles were demonstrated to possess angiogenic properties, attributable to their content of angiogenic growth factors [25]. However, the implications of lipid droplet reduction in grafts and the subsequent activation of inflammatory processes have not been extensively investigated. Furthermore, increased lipid droplet removal during preparation necessitates a substantial level of adipocyte regeneration to offset the resultant volume loss.

In this study, we utilized a mechanical extrusion device to fabricate lipid droplet-free nanovesicles derived from SVF, specifically referred to as SVF-extruded vesicles (SVF-EVs). Subsequently, we performed a comprehensive characterization of the SVF-EVs, emphasizing their particle size, surface labeling, and encapsulated contents. Additionally, we examined the influence of SVF-EVs

on the adipogenic differentiation potential of ADSCs. To investigate a novel and more effective strategy for addressing the challenge of repairing large-volume soft tissue defects, we conducted animal experiments involving the co-transplantation of SVF-EVs and dermal microparticles. We assessed the volume retention rate of the grafts as well as adipocyte regeneration within the central region of the grafts.

Materials and methods

Fabrication of SVF-EVs

Adipose tissue was obtained from donors through liposuction at Wuhan Union Hospital. The samples were washed three times and centrifuged at 700 rpm for 5 min to achieve purification. Subsequently, 10 mL of adipose tissue was transferred into a 20-mL syringe, which was connected to another 20-mL syringe via a Luer-Lock taper, and the contents were repeatedly compressed. The resulting suspension was then centrifuged at 2000 g for 5 min. Following centrifugation, the oil layer was collected and its volume (V1) was measured before disposal. The resulting mixture was then subjected to ultrasonication at 4 ℃ for 5 min, followed by centrifugation at 2000 g for an additional 5 min. Subsequently, the floating cream layer was removed, and its volume (V2) was determined. The total volume (V3) of the discarded lipid droplets was calculated using the equation: V3 = V1 + V2.

The residual fraction underwent a series of five sequential extrusions, as detailed in our previous study [25]. Following storage at 4 °C for a duration of two hours, the sample was subjected to ultracentrifugation at 100,000 g for 70 min at 4 °C. The resulting SVF-EVs were collected in an ultracentrifugal tube and subsequently resuspended in saline for further analysis.

Oil Red O staining of SVF and SVF-EVs were conducted according to the manufacturer's instruction (Solarbio, Beijing, China). Quantitative analysis of the Oil Red O-positive area and diameter was conducted using statistical methods based on data from five randomly selected fields of view obtained with a Nikon microscope.

Characterization of SVF-EVs

The morphology of SVF-EVs was characterized using transmission electron microscopy (TEM, HT7800, HITACHI, Japan) as previous description [26]. Briefly, the resuspension of SVF-EVs was placed onto the grid and then absorbed for 30 min. The grids were fixed with 1% glutaraldehyde for 5 min and stained with uranyl acetate. After drying at room temperature, TEM micrographs were conducted and the morphology of SVF-EVs was examined.

The particle size distribution and concentration of SVF-EVs were assessed using Nanoparticle Tracking Analysis (NTA, NanoSight 300, Malvern Panalytical, UK). The sample was diluted 10^3 times with sterile normal saline and the quantities of diameter and concentration of SVF-EVs were displayed through image visualization.

PKH26, a red fluorescent cell membrane linker, was used to label the fabricated nanovesicles following the manufacturer's instructions (MINI26-1KT, Sigma-Aldrich, USA). Briefly, the SVF-EVs and PKH26 dye were co-incubated for 15 min at 37 ℃, and then the labeled nanovesicles were separated by ultracentrifugation. After processing, the resulting particles were observed by a fluorescence microscope (Ni-E, Nikon, Japan).

Cellular uptake assay

ADSCs were isolated from human adipose using the method described in previous report [27]. Briefly, obtained adipose tissues were washed three times with PBS and digested using 0.2% NB4 collagenase (Sigma, USA) at 37 ℃ for 2 h. Enzyme activity was neutralized with an equal volume of low Dulbecco's Modified Eagle's Medium (DMEM, Hyclone, USA). After centrifugation at 280 g for 5 min, cells from sediment were cultured in DMEM supplemented with 10% fetal bovine serum and 1% Penicillin-Streptomycin at 37 ℃ in a humidified atmosphere containing 5% CO_2. Passage 3–5 ADSCs were used in the following test.

Subsequently, ADSCs were incubated with PKH26-labeled SVF-EVs for 4 h and washed three times with phosphate buffered saline (PBS, Servicebio, Wuhan, China). Then the cells were stained with Calcein Acetoxymethyl Ester (Calcein AM, Beyotime, Shanghai, China) and 4′,6-diamidino-2-phenylindole (DAPI, Beyotime, Shanghai, China) as the manufacturer's instructions described and observed by a laser confocal microscope (A1Si, Nikon, Japan) to explore the fabricated SVF-EVs uptake into cells.

Protein analysis of SVF-EVs

Protein concentration in SVF-EVs

The protein concentration in the fabricated vesicles was quantified by BCA-protein assay following the manufacturer's instruction (Beyotime, Shanghai, China). Briefly, after resuspending with sterile saline, the fabricated SVF-EVs were subjected to the NTA to calculate the number of particles in sample firstly. Then the RIPA Lysis Buffer (Beyotime, Shanghai, China) supplemented with protease inhibitor and phosphatase inhibitor was added to the vesicle sample and evenly blown. The resulting solution was incubated with the indicator in BCA assay kit for 30 min at 37 ℃ and measured the absorbance at 562 nm using a microplate reader (BioTek, USA).

Western blotting

Denatured protein samples of quality of 40 μg were separated by 10% sodium dodecyl sulfate polyacrylamide

gel electrophoresis (SDS-PAGE) and then transferred to PVDF membranes. Each blot was blocked with 5% skimmed milk, and incubated were immunodetected with specific antibodies against PPARγ (Santa, USA), CEBPα (Santa, USA), TSG101 (Abcam, UK), CD81(Abcam, UK), ANG1(Sanying, China) and VEGF (Sanying, China) overnight at 4 °C. The membrane was then incubated with secondary antibodies which were purchased from GeneTex (Irvine, USA). Protein bands were visualized with Amersham Hyperfilm ECL (GE Healthcare, USA).

Effect of SVF-EVs on ADSCs in vitro

Effects on viability of ADSCs

ADSCs were seeded into a 96-well plate at a density of 5×10^3 cells per well and cultured in DMEM complete medium supplemented with SVF-EVs. The protein concentration of SVF-EVs was quantified using a BCA assay for the following dose-response experiment. Subsequently, the SVF-EVs were added to the culture medium to achieve final protein concentrations of 0, 20, and 40 ng/mL, respectively. The culture medium for all groups was refreshed daily. CCK-8 assay was performed at predetermined time points (days 1, 2, 3, and 5) to assess the effects of SVF-EVs on the viability of ADSCs.

Effects on adipogenesis of ADSCs

ADSCs were seeded into a 12-well plate at a density of 2×10^4 cells per well and grown to 50% confluence. The protein concentration of SVF-EVs was determined using BCA assay and then the fabricated vesicles were respectively added to the culture medium to a final protein concentration of 20 ng/mL and 40 ng/mL. The control group received an equal volume of normal saline. The culture medium for all groups was changed every other day. Oil Red O staining was conducted on days 7 and 14 of the culture period according to the manufacturer's instruction (Solarbio, Beijing, China). Briefly, ADSCs at these time points were rinsed twice with PBS and subsequently fixed in 4% paraformaldehyde solution for 20 min. After being immersed in 60% isopropanol for 5 min, the cells were stained with Oil Red O solution for 10 min and rinsed in distilled water three times. Then the hematoxylin staining solution was added to the sample and incubated for 2 min at room temperature. The cells were washed again with distilled water and observed with an inverted aberration microscope (Ts2, Nikon, Japan).

qRT-PCR analysis

Total RNA was extracted from ADSCs cultured for 14 days using a SeraMir RNA purification kit (System Biosciences, CA, USA) and reverse transcribed into cDNA using a cDNA synthesis kit (Thermo Fisher Scientific, OH, USA). qRT-PCR was conducted using AceQ Universal SYBR qPCR Master Mix (Vazyme) following the manufacturer's protocol. Primers used for qRT-PCR analysis are presented in Table 1. The reaction volumes (total 25 μL) contained 5 μL diluted cDNA solution, 10 μL Mix, and 0.4 μL of forward and 0.4 μL of reverse primers. qRT-PCR was performed using the StepOnePlus™ Real-Time PCR System (Applied Biosystems, Thermo Fisher, USA) with the following thermocycling conditions: denaturation at 95 °C for 5 min, followed by 40 cycles of 95 °C for 10 s and 55 °C for 30 s. Relative mRNA expression results were calculated using the $2^{-\Delta\Delta CT}$ method and normalized to *β-actin*.

Western blotting

Western blotting procedure was performed as above outlined. Specifically, the membranes were immunodetected using antibodies targeting PPARγ (Santa, CA, USA), FAS (Santa, CA, USA), ADPN (Santa, CA, USA), and GAPDH (Antgene, Wuhan, China) overnight at 4 °C.

Effect of SVF-EVs on macrophage in vitro

The macrophage line RAW264.7 cells were utilized to verify the impact of SVF-EVs on inflammatory reaction. RAW264.7 cells were seeded into a 6-well plate at a density of 2×10^4 cells per well and cultured in a high-glucose DMEM complete medium. After reaching confluence, the culture medium was refreshed with DMEM, either supplemented with 40 ng/mL SVF-EVs or left unsupplemented. Following a 48- hours incubation, the cell supernatant was harvested and subjected to centrifugation at 3000 r/min for 15 min. Subsequently, the resultant supernatant was meticulously collected and subjected to analysis utilizing an ELISA kit to quantify the concentrations of inflammation-associated cytokines, including IL-6, IL-10, and TNF-α, in accordance with the manufacturer's instructions (Servicebio, Wuhan, China).

Table 1 Primers used for qRT-PCR analysis

Gene name	Primer F	Primer *R*	Accession number	Anneal Temp.	Product Length
β-actin	ACAGAGCCTCGCCTTTGC	AGGGTGAGGATGCCTCTCTT	NM_001101.5	55	255
Homo PPARγ	GACCACTCCCACTCCTTTGA	ATGAGGGAGTTGGAAGGCTC	NM_001354667.3	55	242
Homo FAS	GTGCTGGACCTCTTCCTGAA	CGGATGCCCAGGATGTGT	NM_004104.5	55	134
Homo ADPN	CAGGCCGTGATGGCAGAGATG	GGTTTCACCGATGTCTCCCTTAG	NM_001177800.2	55	92
Homo C/EBPβ	CGCTTACCTCGGCTACCAG	GCTTGTCCACGGTCTTCTTG	NM_001285878.1	55	185

In vivo study

The in vivo study had been conducted in accordance with the ARRIVE guidelines 2.0 which has been uploaded as supplementary material. The objective of this study was to investigate the efficacy of SVF-EVs in facilitating fat regeneration within dermal microparticle tissue. We referred to a widely accepted animal model for fat graft and injected SVF-EVs combined with dermal microparticles into the back subcutaneous region of male nude mice. The volume and weight of grafts in the subcutaneous region of nude mice were systematically recorded at predetermined time points, followed by histological evaluations to address the research objectives. The research protocol for this animal experiment was meticulously developed prior to the study's initiation and received approval from the Animal Ethics Committee of Huazhong University of Science and Technology (HUST).

Based on the pre-experimental results conducted in vitro before animal studies, SVF-EVs demonstrated safety profiles and facilitated adipocyte regeneration in vitro. Considering the above and animal welfare, the animals were allocated into three groups, each comprising eight nude mice for further testing at two time points. Briefly, Four-week-old male BALB/c nude mice, with a weight range of 12–14 g, were procured from Vital River Laboratory Animal Technology Co., Ltd. (Beijing, China). These mice were subsequently housed in specific pathogen-free animal facilities and maintained under standard conditions, with a temperature of 22 ± 2 ℃ and relative humidity between 50 and 70%, following a 12-hour light/12-hour dark cycle. The mice were provided with unrestricted access to standard laboratory water and food. After two days of adaptive feeding, twenty-four ear-tagged nude mice were randomly assigned to three groups using a random number table and the random number remainder grouping method.

Meanwhile, human dermal tissues were collected from discarded excess surgical skin tissue within Wuhan Union Hospital and trimmed into microparticles which could be injected with 18-G needles. After the randomly grouped mice were anesthetized by inhaling an appropriate amount of isoflurane (RWD Life Science Co., LTD, Shenzhen, China), the experimenter performed subcutaneous injections of 0.5 mL of the designated grafts into the dorsal region of the nude mice. The experimental groups were as follows: (1) Control group: received an injection of 0.2 mL of normal saline (0 ng/mL SVF-EVs) combined with 0.3 mL of dermal microparticles; (2) SVF-EVs group: received an injection of 0.2 mL of normal saline containing SVF-EVs encapsulating 20 ng of protein content, along with 0.3 mL of dermal microparticles (final concentration of 40 ng/mL); (3) Lipid droplet group: received an injection of 0.2 mL of lipid droplets derived from adipose tissue, together with 0.3 mL of dermal microparticles. Following recovery, nude mice were maintained in specific pathogen-free animal facilities and provided with unrestricted access to water and food. In the subsequent statistical analysis of the in vivo study, normally developing nude mice would be included. However, if a nude mouse expired or if the subcutaneous graft on its back resulted in skin ulceration and erosion, the sample from that particular nude mouse would be excluded from the study. In our animal experiment, the mice in both the 0 ng/mL group and the 40 ng/mL group were maintained on a standard diet. However, five nude mice in the Lipid droplet group exhibited skin erosion and ulceration, necessitating their exclusion from the study. The excluded animals were humanely euthanized via an overdose of inhaled isoflurane.

After a four-week feeding period, an independent experimental operator, blinded to the group assignments, randomly selected four nude mice from both the Control group and the SVF-EVs group using the random remainder grouping method. These mice were subsequently euthanized via inhalation of an overdose of isoflurane. The grafts were harvested and their weights were measured utilizing an analytical balance (ME204, METTLER, Switzerland), while their volumes were determined via the drainage method. After an additional two-week period, the remaining mice were euthanized, and the weights and volumes of the grafts were assessed using the same methodologies. The specimens were then fixed in paraformaldehyde to facilitate subsequent histological analysis.

Histological evaluation

The harvested samples underwent dehydration through a graded alcohol series and were subsequently embedded in paraffin. The samples were then sectioned into 5 μm thick slices, followed by Hematoxylin and Eosin (HE) staining to delineate the tissue structure. For immunofluorescent staining, the sections were incubated with primary antibodies against perilipin (Abcam, UK) and human-Lamin A/C (Abcam, UK). These were then incubated with PE- and FITC-conjugated goat anti-rabbit IgG antibodies (Servicebio, Wuhan, China), respectively. The nuclei were counterstained with DAPI. Immunofluorescent staining images were analyzed utilizing Image-Pro Plus software (Media Cybernetics, USA), where the area and depth (distance from the edge) of perilipin-positive adipocytes were quantitatively assessed. For immunohistochemical staining, the slides were sequentially incubated with primary antibodies (CD68 and CD206, Abcam, UK) followed by incubation with a secondary antibody, specifically a horseradish peroxidase-conjugated goat anti-rabbit IgG antibody. Histological images were acquired using a Nikon Ni microscope.

Statistical analysis

All data collected in this work were expressed as mean ± SD and analyzed with SPSS 21.0 software (IBM, USA). A Student's t test was used for the comparisons between two groups and a one-way analysis of variance (ANOVA) test with post hoc contrasts by Newman–Keuls test was used to analyze differences in multiple comparisons. $P < 0.05$ was considered to be a statistically significant difference.

Results

Preparation of SVF-EVs from adipose tissue

A schematic of the process of preparing adipose tissue into SVF-EVs is shown in Fig. 1A. Adipose tissue retained the SVF after partial removal of lipid droplets by mechanical shear force, then some of the oil droplets were removed by ultrasound and filter membrane extrusion, and the cell membrane broke and reassembled into nanovesicles, accompanied by multiple active components being encapsulated. Figure 1B showed the macroscopic morphology of SVF retained following mechanical shearing, characterized as a yellow, gel-like substance that still contained oil droplets observable under a microscope. In contrast, Fig. 1C showed that the prepared SVF-EVs appeared clarified and homogeneous upon resuspension in saline, exhibiting no agglutination and an absence of oil droplets. The proportion of discarded oil to the volume of initial adipose tissue was calculated. The mechanical shearing process removed about 71.33 ± 2.08% and the following ultrasound and centrifugation processes further discarded 3.73 ± 0.75%, the total removal ratio was calculated at 75.07 ± 2.80%. Oil Red O

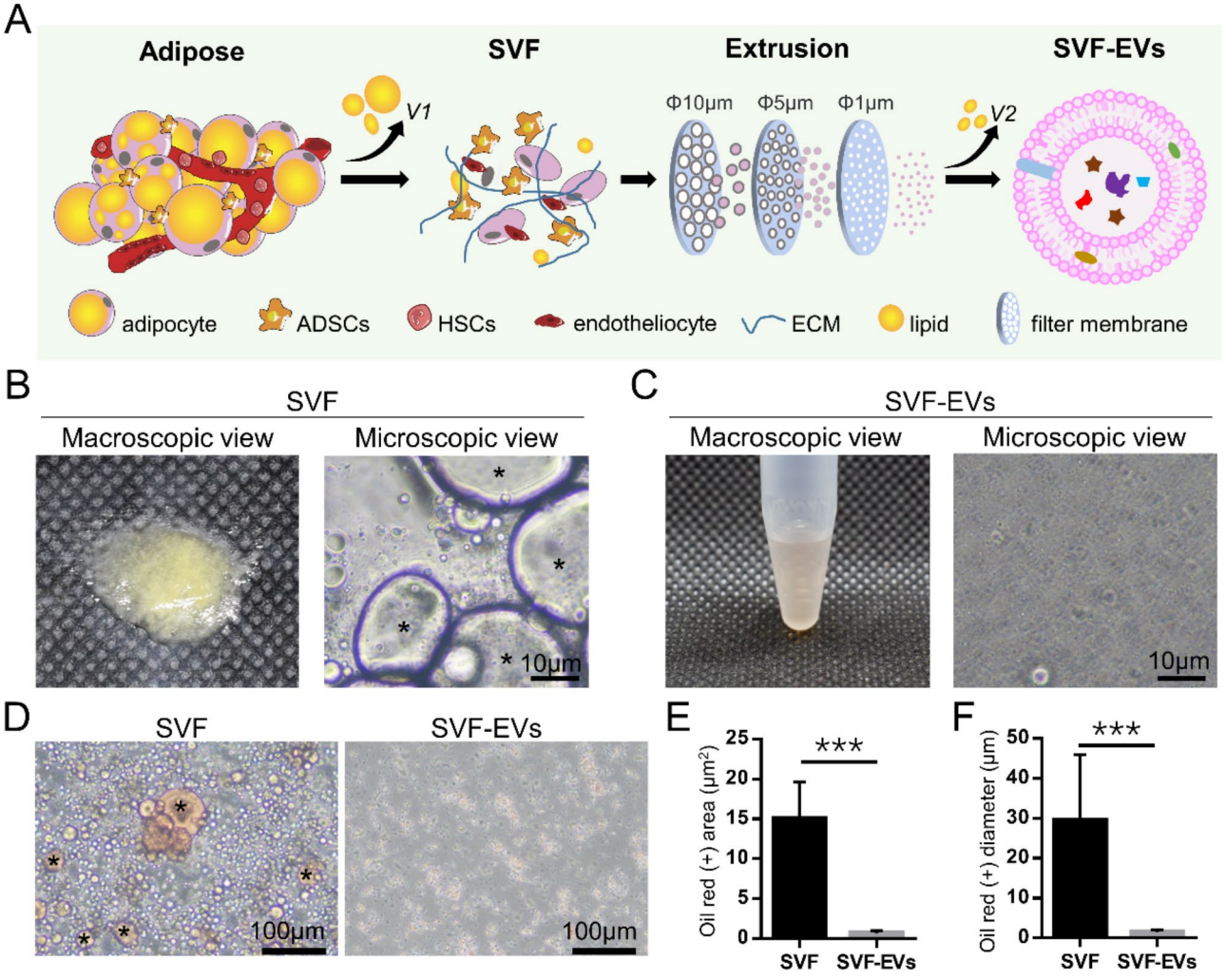

Fig. 1 Schematic illustration of preparation procedure and discarded lipid evaluation of SVF-EVs. **(A)** Illustration of the preparation procedure of SVF-EVs from adipose tissue. Macroscopic and microscopic images of **(B)** SVF and **(C)** SVF-EVs, SVF-EVs resuspended in saline behave homogeneously and clarified. **(D)** Oil Red O staining reveals no obvious lipids in SVF-EVs under the microscope, which is lipid-deficient compared with SVF. Statistical analysis of oil red (+) area **(E)** and diameter **(F)** demonstrated that the gel-like SVF contained stained oil, while nearly lipid droplet-free nanovesicles were seen in SVF-EVs. ($n = 5$, ***: $p < 0.001$, statistical methods: Student's t test)

staining of SVF and SVF-EVs were shown in Fig. 1D, and the relative statistical analysis (Fig. 1E and F) confirmed that the gel-like SVF contained stained oil, whereas the SVF-EVs exhibited nearly lipid droplet-free nanovesicles.

Characteristics of SVF-EVs

According to the analysis of TEM images (Fig. 2A), SVF-EVs were identified as 150 nm spherical vesicles with a bilayer lipid membrane. Identified with the morphological results of the electron microscope, the NTA of SVF-EVs (Fig. 2B) verified the size distribution with a range of diameters around 100–200 nm, and the peak diameter was about 152 nm. Western blot showed that SVF-EVs express tetraspanin proteins, including CD81 and TSG101, as shown in Fig. 2C. The cell membrane dye PKH26 was successfully linked to the membrane of SVF-EVs and displayed red fluorescence (Fig. 2D), confirming that the nanovesicles were reassembled from the broken cell membrane.

After co-cultured with ADSCs, the PKH26-labeled SVF-EVs (red) were internalized into calcein AM-labeled live cells (green) and surrounded the nucleus (blue, Fig. 2E). The particle quantities and protein concentration of prepared SVF-EVs at five different processes were displayed in Fig. 2F, and the linear regression analysis revealed that the total protein concentration is correlated to the number of SVF-EVs ($p = 0.015$). It means that the concentration of proteins encapsulated within each SVF-EV is close after the extant preparation procedure, and therefore we speculate that this preparation process is capable of stabilizing the formation of relatively homogeneous nanovesicles. Western blot analysis (Fig. 2G) revealed that SVF-EVs encapsulate proteins such as PPARγ, C/EBPα, which promotes adipogenesis, and ANG-1, VEGF, which improves angiogenesis.

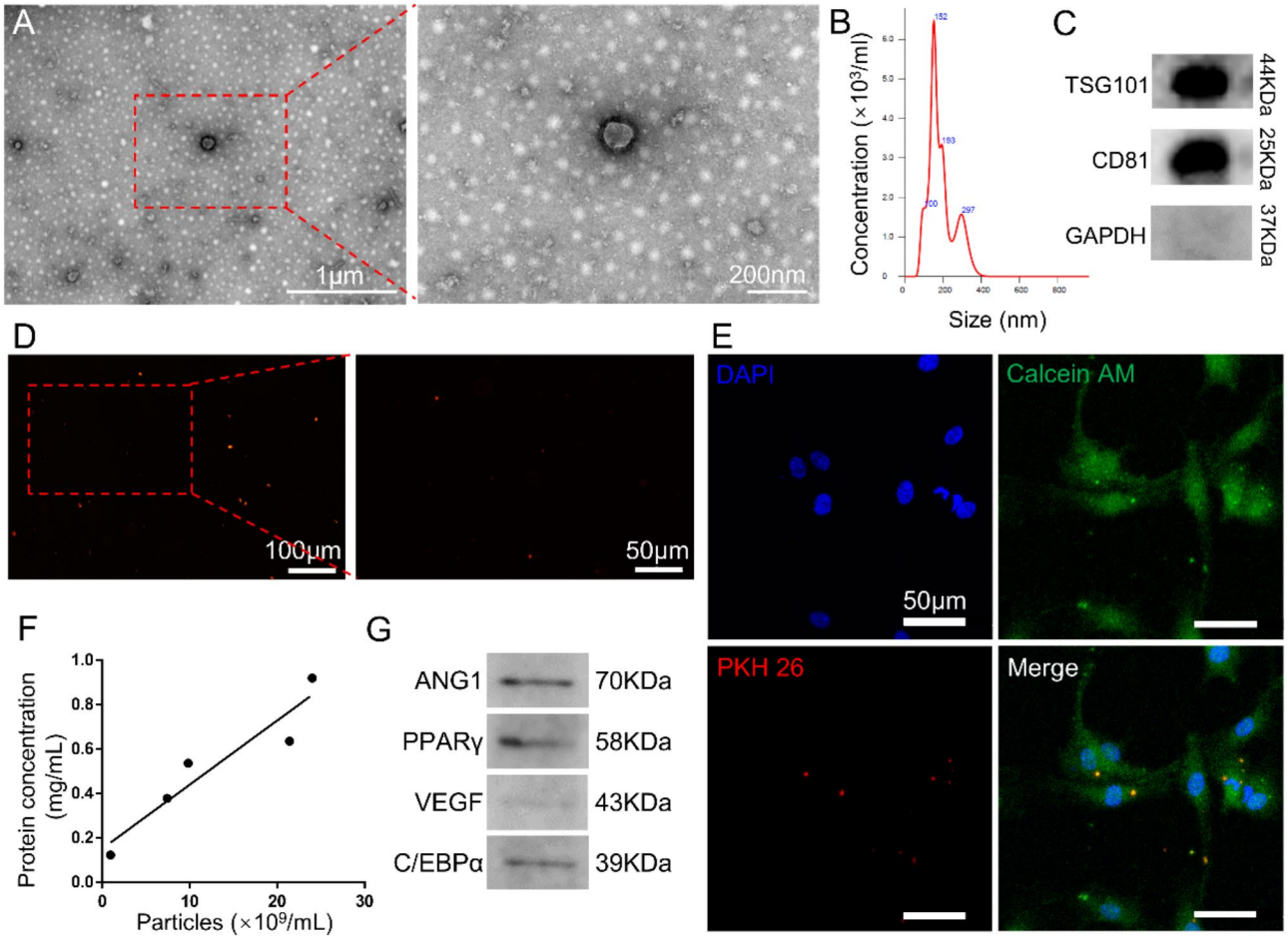

Fig. 2 Characteristics of SVF-EVs. **(A)** TEM images of SVF-EVs. **(B)** NTA analysis of SVF-EVs. The diameter of SVF-EVs is around 100 ~ 200 nm. **(C)** Western blot shows that SVF-EVs express tetraspanin proteins like TSG101 and CD81. **(D)** Fluorescent images show that SVF-EVs could be labeled with PKH26 (red). **(E)** Confocal images verify the internalization of PKH26-labeled SVF-EVs (red) into ADSCs (Calcein CM, green). **(F)** Linear regression analysis investigates the total protein concentration correlated to the number of SVF-EVs. **(G)** Western blot reveals that SVF-EVs encapsulate proteins such as PPARγ, C/EBPα, which promotes adipogenesis of ADSCs. (The uncropped full-length gels and blots were shown in Supplementary Fig. 3)

Effects of SVF-EVs on ADSCs in vitro

Images (Fig. 3A) from the Oil Red O staining and the statistical analysis (Fig. 3B) showed that SVF-EVs promote the lipids synthesis in ADSCs and the amounts of synthetic lipid are correlated to the time and concentration of co-cultured SVF-EVs. Particularly, ADSCs in the blank group had no intracellular lipid droplet formation after 14 days of culture (Fig. 3B), which is consistent with the fact that adipogenic differentiation of ADSCs requires the addition of adipogenic inducers like dexamethasone, insulin, and indomethacin in culture medium. The Oil Red O staining reminded us that 40 ng/mL SVF-EVs could induce significant adipogenic differentiation of ADSCs, but 20 ng/mL SVF-EVs did not. The CCK-8 assay (Fig. 3C) showed that SVF-EVs had no side effects on the growth of ADSCs, and the viability of ADSCs was positively correlated to the concentration of SVF-EVs. Based on the results of the above dose-response experiments, SVF-EVs with a concentration of 40 ng/mL were selected for subsequent adipogenesis-related experiments.

The qRT-PCR showed that the mRNA expression of adipogenic genes such as *PPARγ*, *FAS*, *ADPN*, and *C/EBPβ* in ADSCs treated with 40 ng/mL SVF-EVs were higher than blank control (Fig. 4A-D). Western blot (Fig. 4E) and quantitative analysis of optical density (Fig. 4F) verified the protein levels of PPARγ, FAS, and ADPN were significantly increased in ADSCs treated with 40 ng/mL SVF-EVs.

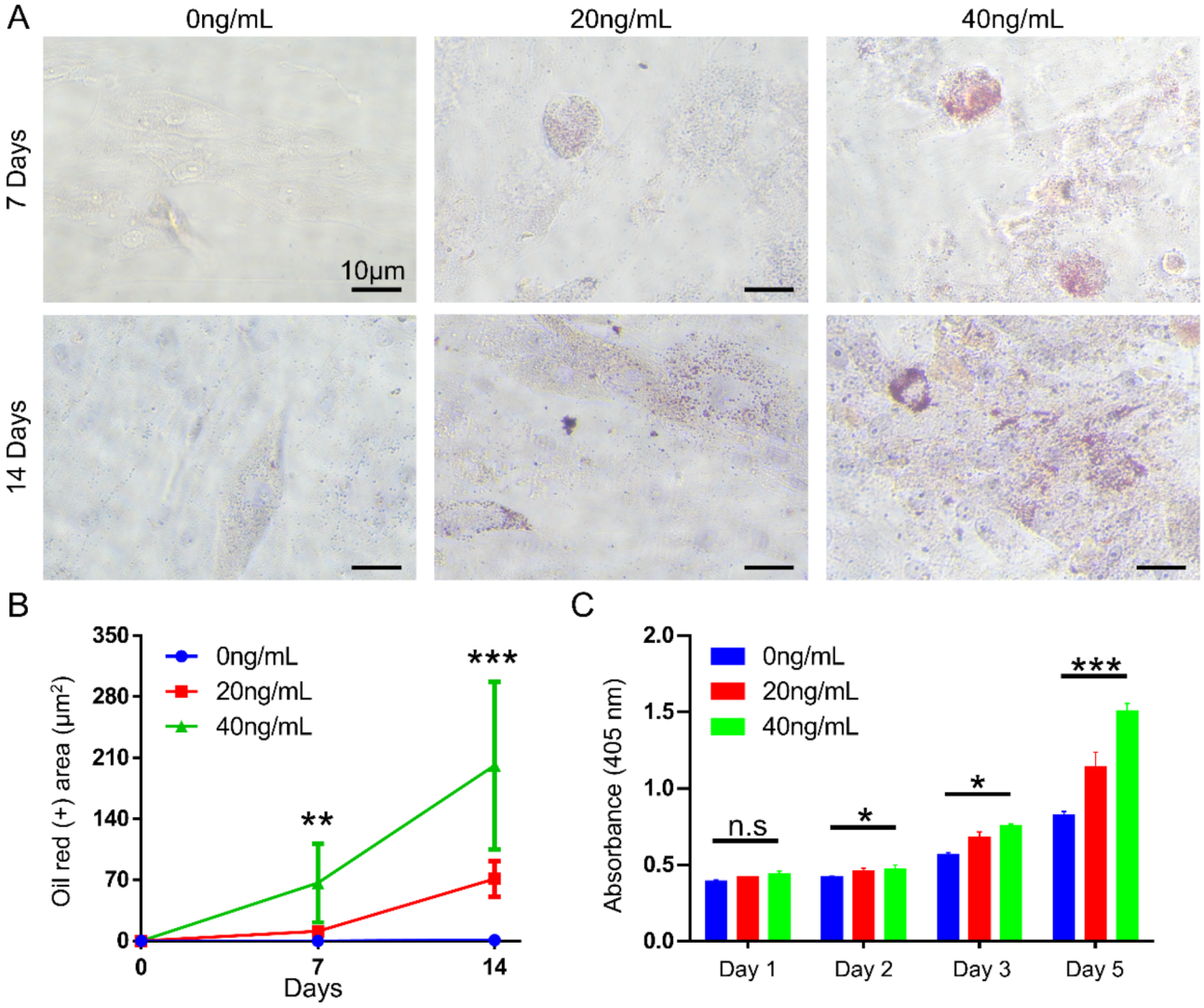

Fig. 3 Effects of SVF-EVs on ADSCs in vitro. **(A)** As evidenced by Oil Red O staining, SVF-EVs promote lipids synthesis in ADSCs, and the amounts of synthetic lipid are correlated to the time and concentration of co-cultured SVF-EVs. **(B)** The statistical analysis of oil red (+) area in staining of ADSCs. **(C)** The CCK-8 assays indicated that SVF-EVs could promote the proliferation of ADSCs. ($n=3$, *: $p<0.05$, **: $p<0.01$, ***: $p<0.001$, n.s: no significance, statistical methods: one-way ANOVA test)

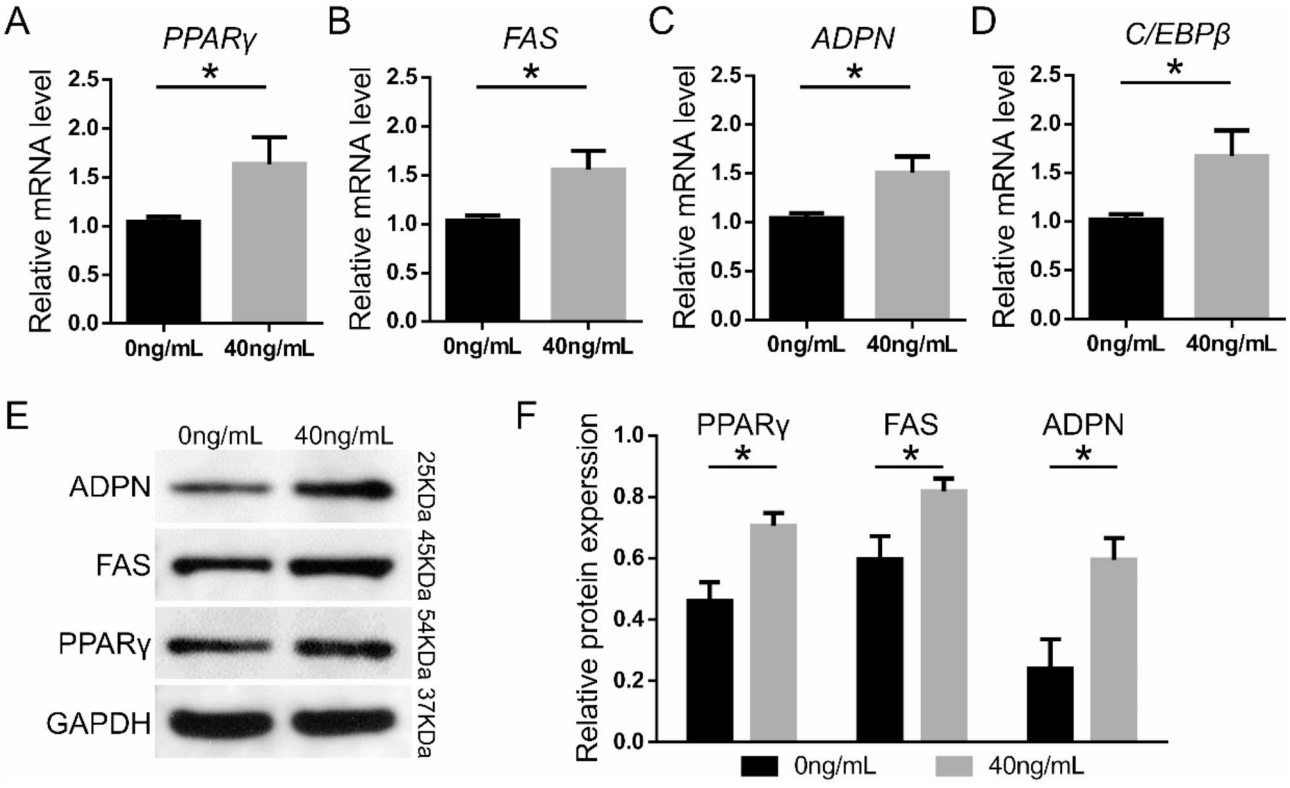

Fig. 4 Effects of SVF-EVs on the adipogenic genes expression in ADSCs. **(A-D)** The relative mRNA expression of adipogenic genes such as *PPARγ*, *ADPN*, *FAS*, and *C/EBPβ* in ADSCs treated with SVF-EVs or blank control. **(E)** Protein levels and **(F)** quantitative analysis of PPARγ, FAS, and ADPN in ADSCs with SVF-EVs or blank stimulation, GAPDH was used as a loading control. ($n = 3$, *: $p < 0.05$, statistical methods: Student's t test. The uncropped full-length gels and blots were shown in Supplementary Fig. 3.)

Effects of SVF-EVs on adipogenesis within the dermal microparticle grafts

Figure 5A and B respectively showed the macroscopic views of the harvested specimens that dermal microparticles were grafted in conjunction with 0 ng/mL and 40 ng/mL SVF-EVs, and the appearance of the graft exhibited no obvious inflammatory reaction area. After 4 weeks of subcutaneous transplantation of dermal microparticles along with 40 ng/mL SVF-EVs, the volume of harvested grafts was 262.67 ± 33.89 mm^3 compared to 212.67 ± 40.95 mm^3 in the control group, which was statistically different between the two groups (Fig. 5C). After being transplanted for 6 weeks, the volume of grafts in 40 ng/mL SVF-EVs was 228.00 ± 24.71 mm^3 and that in control group was 192.83 ± 16.13 mm^3, the difference between the two groups was still statistically significant (Fig. 5C). The weight of grafts in the 40 ng/mL SVF-EVs group after 4 weeks' transplantation was 271.27 ± 30.62 mg and that in blank control group was 233.07 ± 47.93 mg, there existed no significant difference between 40 ng/mL SVF-EVs group and control group (Fig. 5D). However, after 6 weeks of transplantation, the weight of grafts in 40 ng/mL SVF-EVs group was 244.86 ± 28.09 mg, and the control group had a higher graft weight of 280.08 ± 15.12 mg, and the difference was statistically significant.

We carried out HE staining to further visualize the internal changes of grafts, and the grafts appeared as homogeneous eosinophilic stains under the microscope. In 40 ng/mL SVF-EVs group, representative graft images showed a larger volume than the control group, and multiple clustered distributions of vacuolar structures were visible inside (Fig. 6A). When HE staining was performed on grafts after transplantation 6 weeks, we found that such vacuolated structures became more numerous, whereas in blank control group, vacuolated structures were present only at the periphery of the grafts (Fig. 6B). At the same time, the vacuolated structures within the grafts of the 40 ng/mL SVF-EVs group became more evenly distributed, unlike the concentrated distribution in some areas at 4 weeks of transplantation.

To make clear the vacuolated structures in HE staining of the harvested grafts, we further performed immunofluorescent staining for perilipin and found that these structures were adipocytes (Fig. 6C-D). Small-sized with multiple intracellular perilipin-positive structures exhibited that neo-adipocytes were regenerated in grafts. The quantitative analysis (Fig. 6E) of the proportion of perilipin-positive area to total section area showed

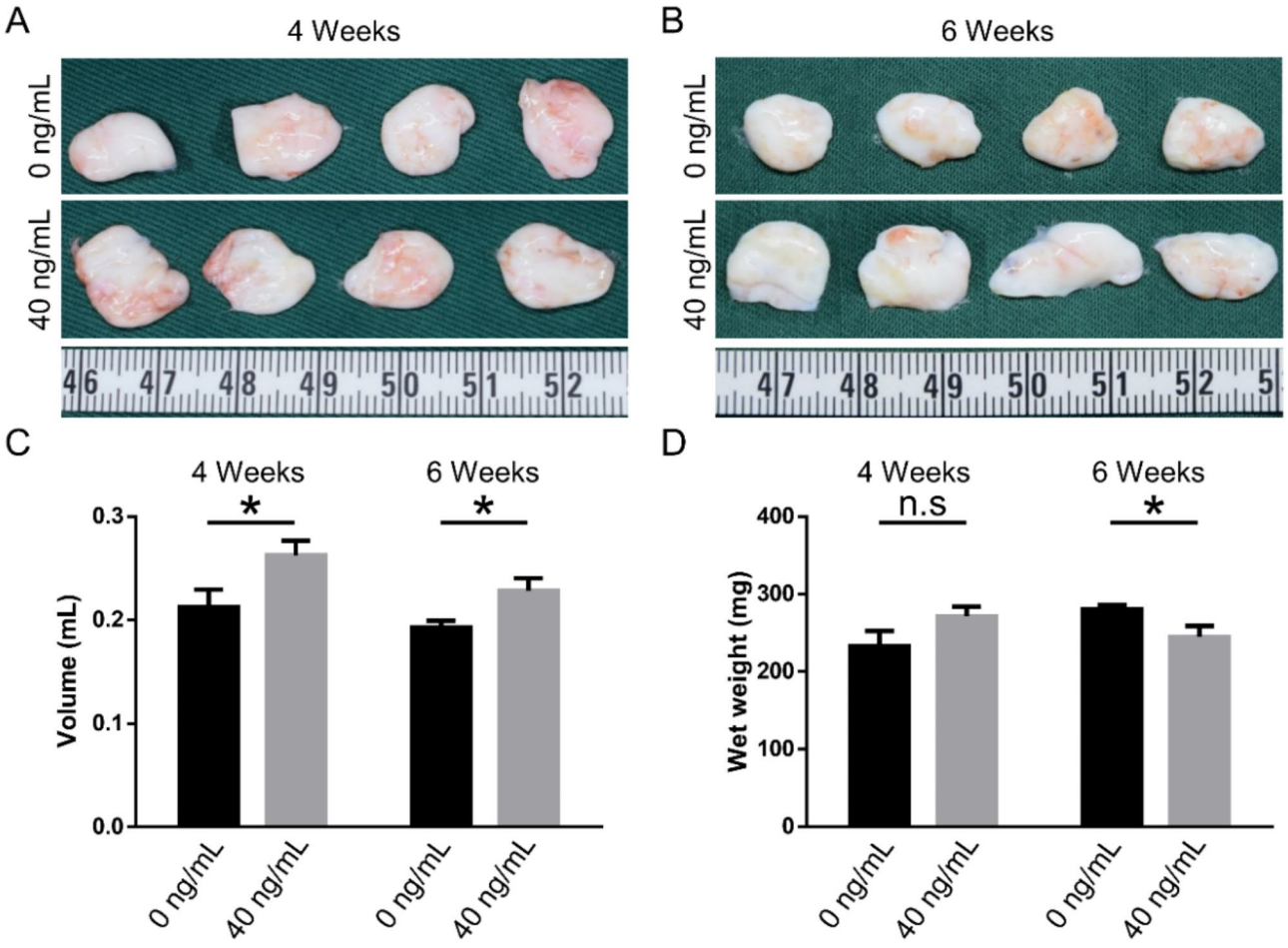

Fig. 5 SVF-EVs enhanced the volume retention rate of grafts in animal test. Macroscopic images of the dermal particle grafts mixed with 0 or 40 ng/mL SVF-EVs after subcutaneous transplanted in nude mice for **(A)** 4 weeks and **(B)** 6 weeks. The quantitative analysis of **(C)** volume and **(D)** wet weight of subcutaneous grafts after transplanted for 4 and 6 weeks. ($n = 4$, *: $p < 0.05$, n.s: no significance, statistical methods: Student's t test)

that grafts in 40 ng/mL SVF-EVs group existed more adipocytes (15.65 ± 9.22%) than that in control group (1.11 ± 0.94%) after 4 weeks' transplantation, and the difference was even more pronounced at 6 weeks (40 ng/mL SVF-EVs group: 22.56 ± 7.49%, blank control group: 1.81 ± 0.82%). The depth of neo-adipocytes to the edge of graft was another considerable parameter reflecting the effect of adipogenesis. As shown in Fig. 6F, neo-adipocyte appeared at the periphery of the grafts in the blank control group at a small depth (702.93 ± 354.47 μm in 4 weeks and 632.43 ± 147.31 μm in 6 weeks), whereas neo-adipocyte regenerated in the central region of grafts in 40 ng/mL SVF group with a large depth (1968.23 ± 668.08 μm in 4 weeks and 3014.34 ± 745.86 μm in 6 weeks). Meanwhile, a comparison of simulated normal distribution (Fig. 6G) of neo-adipocytes' diameter in dermal grafts showed that 40 ng/mL SVF-EVs promoted the regeneration of more large-diameter adipocytes after 6 weeks of co-transplantation, which indicated a higher degree of adipogenesis.

Figure 7 showed the results of staining for perilipin and human-Lamin A/C within the central area of graft using double immunofluorescence labeling. Perilipin-positive (red) regions indicated regenerated adipocytes, and the Lamin A/C-positive cells (green) were labeling human cells brought in during initial dermal microparticles grafting [28].

Histological evaluation of the inflammation caused by SVF-EVs in grafts

Immunohistochemical staining was performed to observe the distribution of CD68 labeled M1-type macrophages and CD206 labeled M2-type macrophages in the graft. The staining results (Fig. 8A, C) and statistical analysis in (Fig. 8B, D) showed that there was no significant difference in the distribution of macrophages in the grafts between the blank control group and 40 ng/mL SVF-EVs group. The representative macroscopic images of dermal grafts in blank control group and 40 ng/mL SVF-EVs group were similar, the surface of the graft was

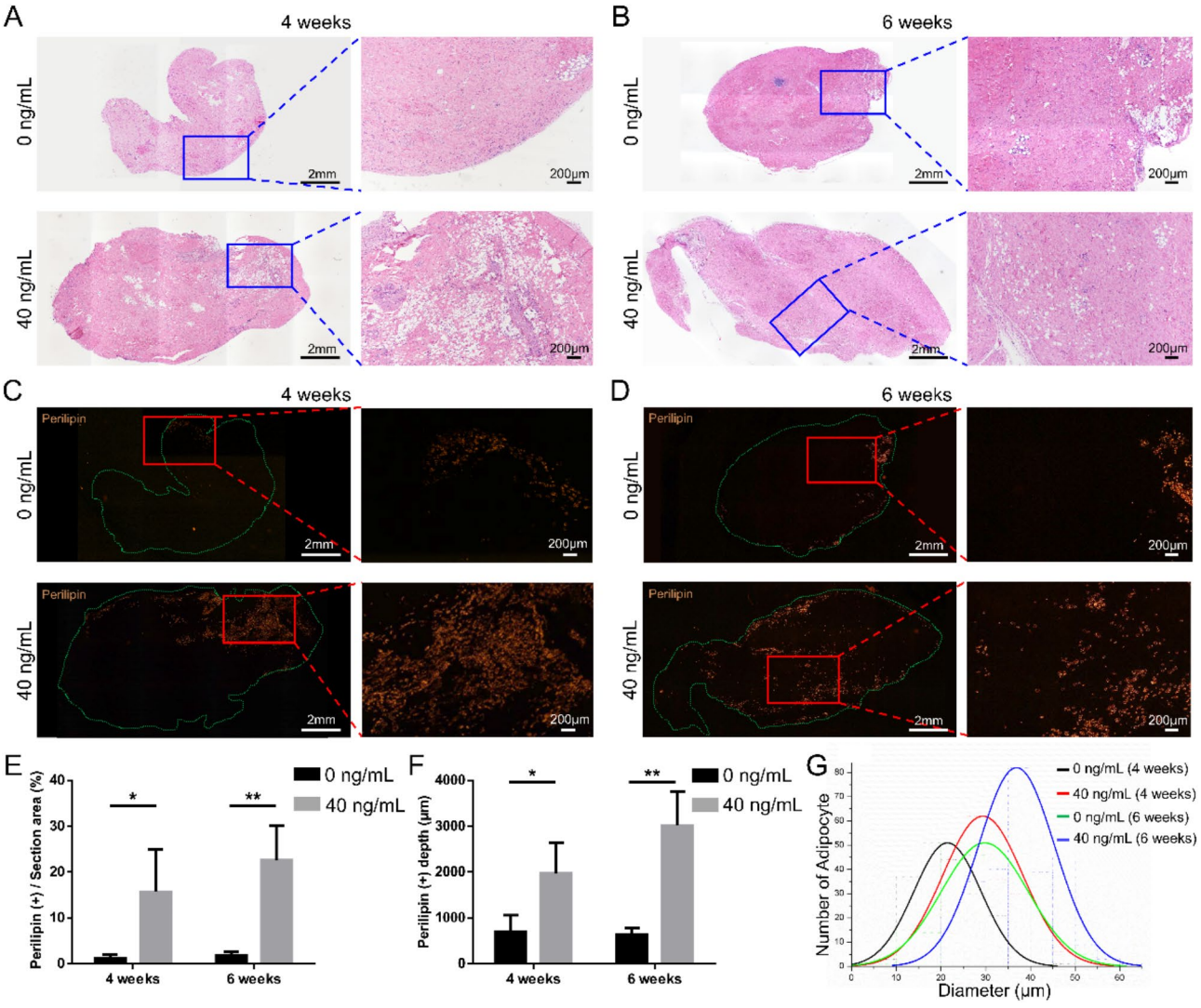

Fig. 6 SVF-EVs promote the neo-adipocyte regeneration in the central of grafts. The overall view of HE staining of grafts after transplantation for 4 weeks **(A)** and 6 weeks **(B)**. Immunofluorescent staining for perilipin of grafts after transplantation for 4 weeks **(C)** and 6 weeks **(D)** to determine adipocyte (gold) regeneration. The quantitative analysis of **(E)** the area and **(F)** infiltration depth of neo-adipocyte (perilipin positive) reveal that SVF-EVs promote adipogenesis in grafts ($n = 4$, *: $p < 0.05$, **: $p < 0.01$, statistical methods: Student's t test). (**G**) The simulated normal distribution of neo-adipocytes' diameter in dermal grafts showed that the diameter of regenerated adipocytes increased with the increase of SVF-EVs concentration and transplantation time

smooth and consistent in texture, with no obvious hyperemia. But when evaluating the grafts harvested from dermal microparticles and lipid droplet co-transplantation, the cyst and surface inflammatory congestion in macroscopic pictures, and the cavity and necrosis in HE staining images all indicated obvious inflammatory changes in grafts (Supplementary Fig. 1).

To enhance the evidence supporting the role of SVF-EVs in attenuating macrophage-mediated inflammatory responses in grafts, we conducted supplementary in vitro ELISA experiments. These experiments quantified the secretion of inflammation-related cytokines by RAW264.7 cells treated with 40 ng/mL of SVF-EVs, followed by statistical analysis. The findings (Supplementary Fig. 2) indicated that treatment with SVF-EVs resulted in an increased secretion of anti-inflammatory cytokines and a decreased secretion of pro-inflammatory cytokines by RAW264.7 cells.

Discussion

For the repair of large-volume soft tissue defects, the depletion of grafts mass during preparation seems to be contradictory to the need for large-volume grafts. Improving post-transplant adipocyte regeneration is an important way to increase the volume retention of autologous soft tissue grafts [29, 30]. It was shown that the activation of ADSCs or preadipocytes by transcription factors PPARγ and C/EBPα regulates increased expression of lipogenic genes such as *Scd*, *Fabp4*, *Pepck*, *Glut4*, *Lpl*, etc., cellular synthesis of lipid-forming enzymes like

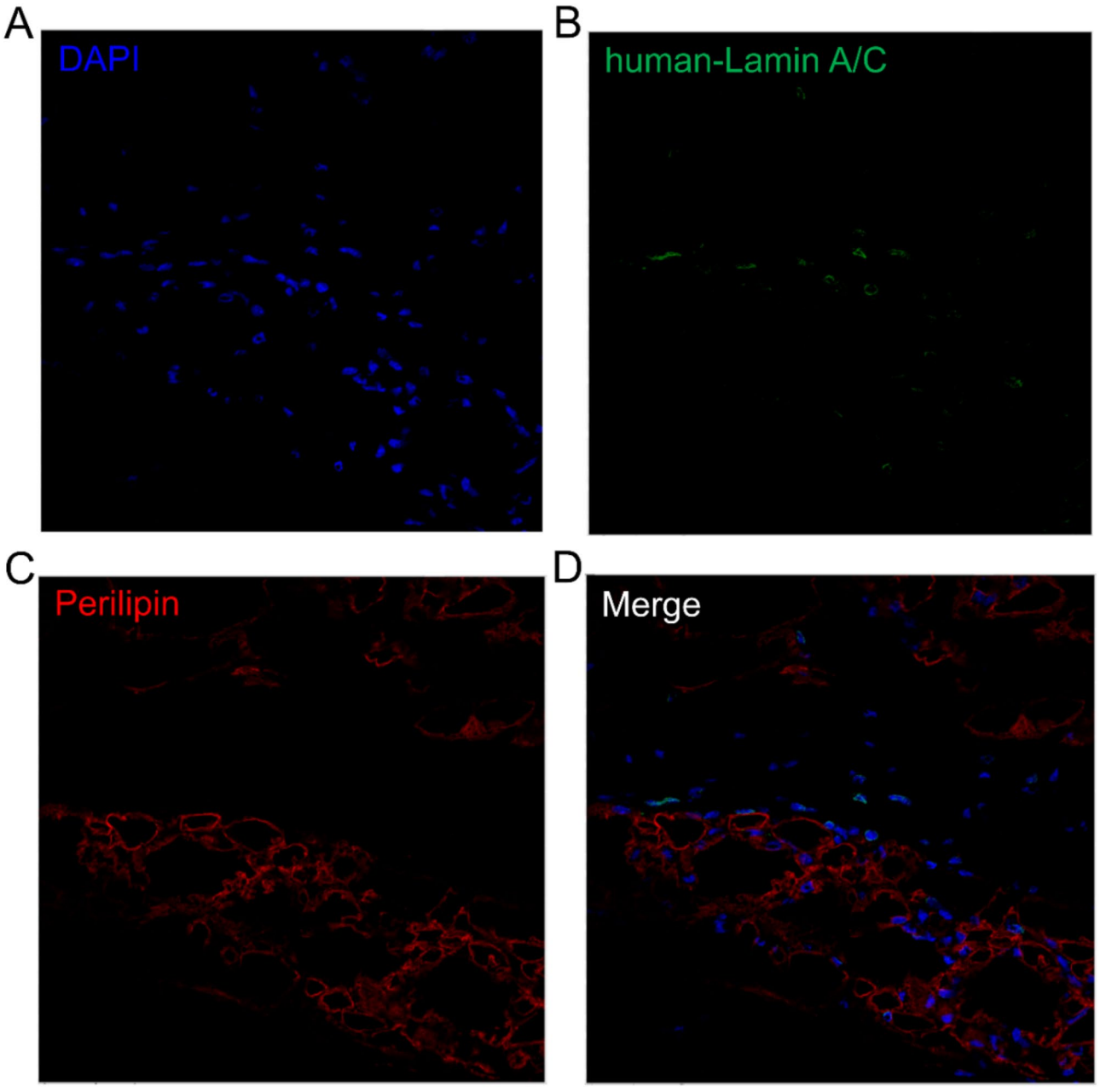

Fig. 7 Histological Evaluation of cell origin of new adipocytes in grafts. Immunofluorescent staining showed that cells positive for human-specific nuclear antibody (anti-Lamin A/C, green) labeling are not present within the perilipin-labeled (red) adipocyte region

glucose transporter, lipoprotein lipase, searyl-CoA-desaturase and fatty acid synthase, and lipid droplets appear in the cells and gradually accumulate, eventually differentiating to form mature adipocytes [31]. Compared to other tissue cells, PPARγ is higher in mature adipocytes [32]. The process of preparing SVF-EVs involves a mechanism that effectively preserves and encapsulates PPARγ within their nanoscale structures. The relative higher presence of PPARγ may underlie the vesicles' capacity to facilitate the regeneration of adipocytes [33, 34]. The result indicates the favorable preservation characteristics exhibited by SVF-EVs, thereby enhancing their suitability for repeated applications.

Tonnard et al. concluded the application of mechanical shear serves as an effective mean to separate lipid droplets from adipocytes within adipose tissue, without compromising the viability and functionality of vital cellular components like ADSCs, endothelial progenitor cells, and hematopoietic progenitors [35]. This approach has been empirically validated through clinical settings, particularly in nano-fat and SVF-gel grafting procedures, where enhanced volume retention rates have been

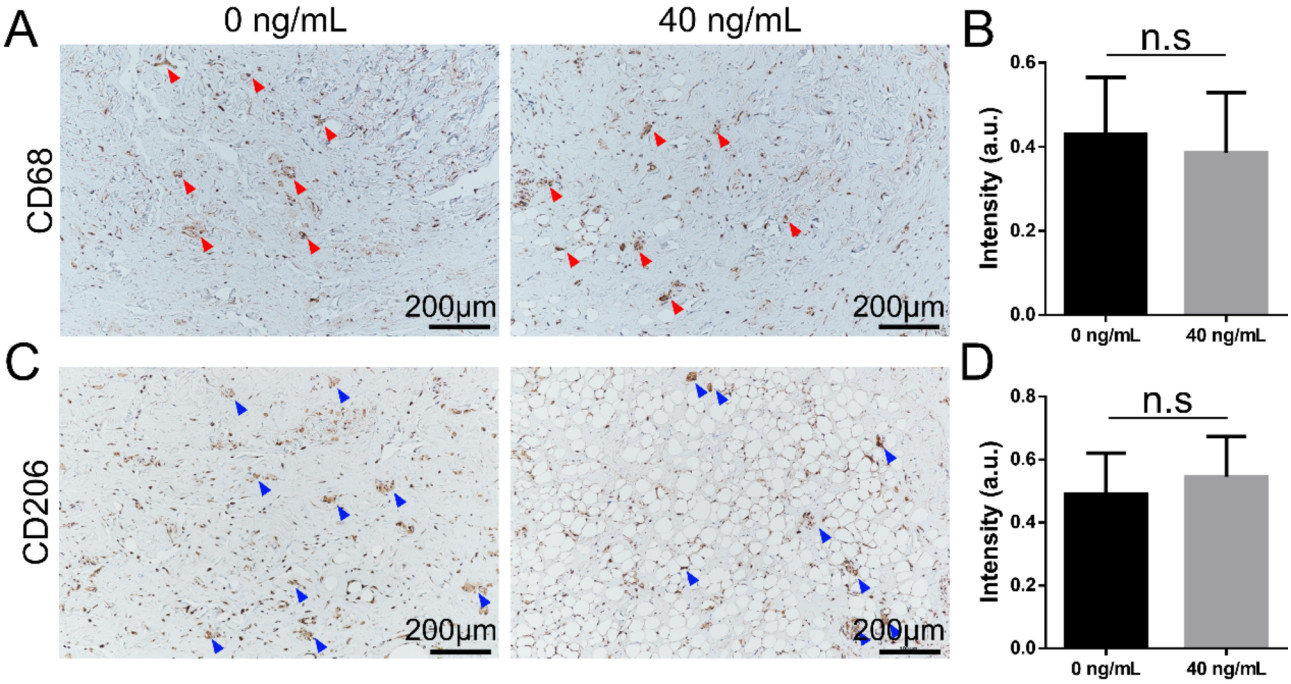

Fig. 8 Histological evaluation of inflammation in grafts. Immunohistochemical staining **(A)** and statistical analysis **(B)** for CD68 of grafts revealed that SVF-EVs did not induce increased numbers and infiltration of M1-type macrophages within the grafts after 4 weeks. The immunohistochemical staining images **(C)** and statistical analysis **(D)** for CD206 of grafts showed that SVF-EVs did not cause increased numbers and infiltration of M2-type macrophages within the grafts after 4 weeks. ($n = 5$, n.s: no significance, statistical methods: Student's t test)

observed [36, 37]. In this study, we purified SVF through back-and-forth squeezing, initially separating and removing 80% of the lipid droplet from the adipose tissue. Following the application of ultrasonication and subsequent passage through filters with varying pore sizes, a significant proportion of 15% of the lipid droplet underwent continued removal, indicating an effective lipid-purification process. When compared to the graft in the control group, the graft combined with SVF-EVs exhibited a similar level of inflammatory cell infiltration. Additionally, the tissue staining revealed well-organized structures and did not provoke a significant inflammatory response, indicating favorable biocompatibility of the SVF-EVs. We employed a positive control group where the dermal microparticles graft, when integrated with lipid droplets, manifested characteristic features such as surface hyperemia, the intra-formation of lipid-droplet cysts, and a pronounced inflammatory response characterized by a surge in both CD68 (+) M1 macrophages and CD206 (+) M2 macrophages. Previous studies have demonstrated that inflammatory factors and fibrous connective tissue formation influence adipocyte differentiation and regeneration [7, 38]. By removing the lipid droplet that causes the inflammatory response, the SVF-EVs reduce these hindering factors and facilitate the regeneration of adipose tissue in the grafts.

To validate the adipogenic potential of SVF-EVs in animal models, we employed dermal microparticles tissue as the carrier matrix for implantation in this study. Because of its ubiquitous presence throughout the human anatomy, abundant availability, and straightforward accessibility, the dermis represents a favored autologous tissue routinely utilized in surgical procedures aimed at volume augmentation [39]. The excised dermal strips are converted into microparticles for grafting, which is more conducive to tissue survival after transplantation [40]. Dermal microparticles can mix well with SVF-EVs and the vesicles are more evenly distributed in the graft. It provides the vehicle and space for the extruded vesicles to function and serves as a protection against diffuse loss of vesicles and straightforward engulfment by the body's immune system [41]. Meanwhile, when the dermal bulk was prepared into microparticle style, the mechanical strength of the graft dermal tissue was found to be reduced more than 10 times as measured in compression tests, and the fluidity of the microparticle form was easier to use in injections [40]. Previous literature showed that mechanical strength was also an important factor in the regeneration of adipose tissue and that an elastic modulus similar to that of natural adipose tissue was more conducive to adipocyte regeneration [42, 43].

In the animal experiments, new adipose tissue was born inside the graft 4 weeks after transplantation, and the graft also showed a decrease in volume over time, with a volume retention rate of 70% at 6 weeks, which is higher than the volume retention rate after fat transplantation

alone. Analyzing the results at two time points, 4 weeks and 6 weeks after transplantation, we found an increase in graft volume but a lower corresponding weight compared to the control group. It suggests that this may be due to the greater amount of less dense adipose tissue produced within the grafts at 6 weeks, whereas dense fibrous connective tissue fills formed within the control group. This was echoed in histological HE staining and perilipin immunofluorescence staining. An important improvement of in vivo study is to set up more control groups, such as SVF and extracellular vesicles secreted by ADSCs, which can provide more sufficient data when further analyzing and verifying the relevant mechanisms, thus enhancing the future clinic application. Moreover, due to the unexpected skin erosion and necrosis caused by the inflammatory reaction caused by lipid droplets, the relevant specimens were directly excluded from the study and lost the significance of analysis and verification, which is one of the shortcomings of this experiment.

The immunofluorescence staining analysis of the specimens unveiled a distinct pattern of adipose tissue regeneration. Originating from the peripheral regions of the graft, novel adipocyte progressively regenerated towards the graft's interior, with a concomitant increase in the depth of newly formed adipocytes over the course of the grafting period. Subsequent to free tissue transplantation, the paucity of internal vascularization necessitated the reliance on tissue fluid infiltration to supply oxygen, nutrients, and facilitate metabolic exchange within the graft's interior [4]. This condition significantly influenced the spatial distribution and directionality of adipose tissue regeneration within the graft. Scholarly discourse posits the presence of stem cells within dermal tissue, classified as preadipocytes that have been experimentally validated to differentiate into adipose tissue [44]. In our experiment, we employed anti-human nuclear antibodies (human Lamin A/C) to fluorescently tag cells within the dermal tissue. Our findings revealed a non-overlapping pattern between the regenerated adipocytes within the graft and the cells introduced via dermal microparticles, suggesting that the nascent adipocytes likely differentiated from host nude mouse cells post-transplantation. Based on the result presented in Fig. 3, we formulated a hypothesis wherein subcutaneous cells of nude mice migrated into the graft and, under the influence of SVF-EVs, underwent differentiation into adipocytes. However, the precise mechanism underlying the SVF-EVs mediated migration of exogenous stem cells toward the central region of the graft requires further elaboration.

Conclusion

In summary, SVF-EVs are nanoscale lipid droplet-free vesicles derived from stromal vascular fraction, and their contents contain proteins such as PPARγ, C/EBPα, which facilitate adipogenesis. It has exhibited the ability to promote the adipogenic differentiation of ADSCs in vitro, and facilitate adipocyte regeneration in the centre, and attenuate the inflammatory response of grafts in animal experiments. Our study suggests the potential of SVF-EVs prepared by physical procedure to improve volume retention in autologous grafting. Additionally, SVF-EVs combined with dermal microparticles transplantation is an estimable strategy for repairing large-volume soft tissue defects.

Supplementary Information

The online version contains supplementary material available at https://doi.org/10.1186/s13287-025-04240-6.

Supplementary Material 1: Macroscopic view and HE staining evaluation of grafts harvested from the dermis and lipid droplet co-transplantation (black triangle: oil droplet; red triangle: inflammation and necrosis; *: cavity).

Supplementary Material 2: Statistical analysis of the concentration of inflammatory-associated cytokines secreted by RAW264.7 cells following treatment with either 0 or 40 ng/mL of SVF-EVs. (n=5, *: $p < 0.05$, n.s: no significance, statistical methods: Student's t test.)

Supplementary Material 3

Supplementary Material 4

Acknowledgements

Not applicable.

Author contributions

Jiaming Sun and Jie Yang contributed to the study conception and design. Material preparation, data collection and analysis were performed by Yuyang Zeng and Di Sun. Results visualization was performed by Rongrong Wang and Ran An. The first draft of the manuscript was written by Yuyang Zeng, all authors commented on previous versions of the manuscript. All authors read and approved the final manuscript.

Funding

This work was supported by the National Key R&D Program of China (2019YFA0110500) and the Science Foundation of Tongji hospital (2022B35).

Data availability

The data will be made available on reasonable request, and all additional files are included in the manuscript. The authors declare that they have not use AI-generated work in this manuscript.

Declarations

Ethics approval and consent to participate

Ethical approval was obtained from the Medical Ethics Committee of Union Hospital and the Experimental Animal Ethics Committee of Huazhong University of Science and Technology before the commencement of the study, and the participants provided written informed consent for the use of fat samples. Title of the approved project: Engineered nanovesicles derived from autologous SVF for oil-free adipose tissue regeneration and its mechanism study. Approval Number: [2021] IEC(155). Date of approval: 2 March 2021.

Consent for publication

The manuscript is approved by all authors for publication.

Competing interests

No conflict of interest exit in the submission of this manuscript.

Author details
[1]Department of Plastic Surgery, Union Hospital, Tongji Medical College, Huazhong University of Science and Technology, Wuhan 430022, China
[2]Department of Dermatology, Tongji Hospital, Tongji Medical College, Huazhong University of Science and Technology, Wuhan 430030, China
[3]Wuhan Clinical Research Centre for Superficial Organ Reconstruction, Wuhan 430022, China

Received: 14 October 2024 / Accepted: 17 February 2025
Published online: 05 March 2025

References

1. Debuc B, Gendron N, Cras A, et al. Improving autologous fat grafting in regenerative surgery through stem Cell-Assisted Lipotransfer. Stem Cell Rev Rep. 2023;19(6):1726–54.
2. Pu LL, Yoshimura K, Coleman SR. Fat grafting: current concept, clinical application, and regenerative potential, part 1. Clin Plast Surg. 2015;42(2):ix–x.
3. Pu LL, Yoshimura K, Coleman SR. Fat grafting: current concept, clinical application, and regenerative potential, part 2. Preface. Clin Plast Surg. 2015;42(3):xiii–xiv.
4. Pu LL. Mechanisms of fat graft survival. Ann Plast Surg. 2016;77(Suppl 1):S84–6.
5. Laloze J, Varin A, Gilhodes J, et al. Cell-assisted Lipotransfer: friend or foe in fat grafting? Systematic review and meta-analysis. J Tissue Eng Regen Med. 2018;12(2):e1237–50.
6. Chen Q, Liu S, Cao L, Yu M, Wang H. Effects of macrophage regulation on fat grafting survival: improvement, mechanisms, and potential application-A review. J Cosmet Dermatol. 2022;21(1):54–61.
7. Mineda K, Kuno S, Kato H, et al. Chronic inflammation and progressive calcification as a result of fat necrosis: the worst outcome in fat grafting. Plast Reconstr Surg. 2014;133(5):1064–72.
8. Cai J, Feng J, Liu K, Zhou S, Lu F. Early macrophage infiltration improves fat graft survival by inducing angiogenesis and hematopoietic stem cell recruitment. Plast Reconstr Surg. 2018;141(2):376–86.
9. Yoshimura K, Coleman SR. Complications of fat grafting: how they occur and how to find, avoid, and treat them. Clin Plast Surg. 2015;42(3):383–ix.
10. Chen K, Xiong J, Xu S, et al. Adipose-Derived stem cells exosomes improve fat graft survival by promoting prolipogenetic abilities through Wnt/β-Catenin pathway. Stem Cells Int. 2022;2022:5014895.
11. Zhang Y, Liu T. Adipose-derived stem cells exosome and its potential applications in autologous fat grafting. J Plast Reconstr Aesthet Surg. 2023;76:219–29.
12. Yoshimura K, Sato K, Aoi N, Kurita M, Hirohi T, Harii K. Cell-Assisted Lipotransfer for cosmetic breast augmentation: supportive use of Adipose-Derived stem/stromal cells. Aesthetic Plast Surg. 2020;44(4):1258–65.
13. Chen X, Yan L, Guo Z, et al. Adipose-derived mesenchymal stem cells promote the survival of fat grafts via crosstalk between the Nrf2 and TLR4 pathways. Cell Death Dis. 2016;7(9):e2369.
14. Bora P, Majumdar AS. Adipose tissue-derived stromal vascular fraction in regenerative medicine: a brief review on biology and translation. Stem Cell Res Ther. 2017;8(1):145.
15. Yao Y, Cai J, Zhang P, et al. Adipose stromal vascular fraction gel grafting: A new method for tissue volumization and rejuvenation. Dermatol Surg. 2018;44(10):1278–86.
16. Deng C, He Y, Feng J, et al. Extracellular matrix/stromal vascular fraction gel conditioned medium accelerates wound healing in a murine model. Wound Repair Regen. 2017;25(6):923–32.
17. Cai Y, Zhang F, Feng J, et al. Long-term follow-up and exploration of the mechanism of stromal vascular fraction gel in chronic wounds. Stem Cell Res Ther. 2023;14(1):163.
18. Yao Y, Dong Z, Liao Y, et al. Adipose extracellular matrix/stromal vascular fraction gel: A novel adipose Tissue-Derived injectable for stem cell therapy. Plast Reconstr Surg. 2017;139(4):867–79.
19. Zanata F, Bowles A, Frazier T, et al. Effect of cryopreservation on human adipose tissue and isolated stromal vascular fraction cells: in vitro and in vivo analyses. Plast Reconstr Surg. 2018;141(2):e232–43.
20. Yang Z, Dong L, Jin S, Han X, Li F. Comparison of microfat, Nanofat, and extracellular matrix/stromal vascular fraction gel for skin rejuvenation: basic animal research. Aesthet Surg J. 2023;43(7):NP573–86.
21. Zhang T, Zheng X, Lin R, et al. Lyophilizable stem Cell-Hybrid liposome with Long-Term stability and high targeting capacity. Adv Healthc Mater. 2024;13(22):e2400704.
22. Yoon J, Jo W, Jeong D, Kim J, Jeong H, Park J. Generation of nanovesicles with sliced cellular membrane fragments for exogenous material delivery. Biomaterials. 2015;59:12–20.
23. Wang P, Wang X, Luo Q, et al. Fabrication of red blood Cell-Based multimodal theranostic probes for second Near-Infrared window fluorescence Imaging-Guided tumor surgery and photodynamic therapy. Theranostics. 2019;9(2):369–80.
24. Wen Y, Fu Q, Soliwoda A, et al. Cell-derived nanovesicles prepared by membrane extrusion are good substitutes for natural extracellular vesicles. Extracell Vesicle. 2022;1:100004.
25. Tu J, Zeng Y, An R, Sun J, Wen H. Engineered nanovesicles from stromal vascular fraction promote angiogenesis and adipogenesis inside decellularized adipose tissue through encapsulating growth factors. Sci Rep. 2023;13(1):750.
26. Du Y, Chen Y, Li F, Mao Z, Ding Y, Wang W. Genetically engineered cellular nanovesicle as targeted DNase I delivery system for the clearance of neutrophil extracellular traps in acute lung injury. Adv Sci (Weinh). 2023;10(32):e2303053.
27. Sun D, Mou S, Chen L, et al. High yield engineered nanovesicles from ADSC with enriched miR-21-5p promote angiogenesis in adipose tissue regeneration. Biomater Res. 2022;26(1):83.
28. Xie X, Wu S, Mou S, Guo N, Wang Z, Sun J. Microtissue-Based Bioink as a chondrocyte microshelter for DLP Bioprinting. Adv Healthc Mater. 2022;11(22):e2201877.
29. Zhang Y, Cai J, Zhou T, Yao Y, Dong Z, Lu F. Improved Long-Term volume retention of stromal vascular fraction gel grafting with enhanced angiogenesis and adipogenesis. Plast Reconstr Surg. 2018;141(5):e676–86.
30. Lei C, Cai B, Chen X, Huang Z, Wang B. Introduction of ligated vessels promote the retention and regeneration of free fat: constructing a fat flap in tissue engineering chamber. Adipocyte. 2020;9(1):108–15.
31. de Mota P, Richard AJ, Hang H, Stephens JM. Transcriptional regulation of adipogenesis. Compr Physiol. 2017;7(2):635–74.
32. Ali AT, Hochfeld WE, Myburgh R, Pepper MS. Adipocyte and adipogenesis. Eur J Cell Biol. 2013;92(6–7):229–36.
33. Giuliani G, Rosina M, Reggio A. Signaling pathways regulating the fate of fibro/adipogenic progenitors (FAPs) in skeletal muscle regeneration and disease. FEBS J. 2022;289(21):6484–517.
34. Janani C, Ranjitha Kumari BD. PPAR gamma gene–a review. Diabetes Metab Syndr. 2015;9(1):46–50.
35. Ghiasloo M, Lobato RC, Díaz JM, Singh K, Verpaele A, Tonnard P. Expanding clinical indications of mechanically isolated stromal vascular fraction: A systematic review. Aesthet Surg J. 2020;40(9):NP546–60.
36. Zhang K, Liu F, Zhang Y, et al. Mechanical Vibration-Extracted stromal vascular fraction improves volume retention after autologous fat grafting. Plast Reconstr Surg. 2020;146(6):1275–84.
37. Anudeep TC, Jeyaraman M, Muthu S, et al. Advancing regenerative cellular therapies in Non-Scarring alopecia. Pharmaceutics. 2022;14(3):612.
38. Li Y, Chen S, Sun J, Yu Y, Li M. Interleukin-38 inhibits adipogenesis and inflammatory cytokine production in 3T3-L1 preadipocytes. Cell Biol Int. 2020;44(11):2357–62.
39. Nagano H, Mizuno N, Sato H, et al. Skin graft with dermis and appendages generated in vivo by cell competition. Nat Commun. 2024;15(1):3366.
40. Bassetto F, Turra G, Salmaso R, Lancerotto L, Del Vecchio DA. Autologous injectable dermis: a clinical and histological study. Plast Reconstr Surg. 2013;131(4):e589–96.
41. Wu K, He C, Wu Y, et al. Preservation of small extracellular vesicle in gelatin methacryloyl hydrogel through reduced particles aggregation for therapeutic applications. Int J Nanomed. 2021;16:7831–46.
42. Xie J, Zhang D, Zhou C, Yuan Q, Ye L, Zhou X. Substrate elasticity regulates adipose-derived stromal cell differentiation towards osteogenesis and adipogenesis through β-catenin transduction. Acta Biomater. 2018;79:83–95.
43. Goelzer M, Dudakovic A, Olcum M, et al. Lamin A/C is dispensable to mechanical repression of adipogenesis. Int J Mol Sci. 2021;22(12):6580.
44. Plikus MV, Guerrero-Juarez CF, Ito M, et al. Regeneration of fat cells from myofibroblasts during wound healing. Science. 2017;355(6326):748–52.

Publisher's note